Gene expression profiling of astaxanthin and fatty acid pathways in *Haematococcus pluvialis* in response to different LED lighting conditions

Ruijuan Ma, Skye R. Thomas-Hall, Elvis T. Chua, Faisal Alsenani, Eladl Eltanahy, Michael E. Netzel, Gabriele Netzel, Yinghua Lu, Peer M. Schenk

PII: S0960-8524(17)32098-9
DOI: https://doi.org/10.1016/j.biortech.2017.11.094
Reference: BITE 19244

To appear in: *Bioresource Technology*

Received Date: 18 October 2017
Revised Date: 23 November 2017
Accepted Date: 27 November 2017

Please cite this article as: Ma, R., Thomas-Hall, S.R., Chua, E.T., Alsenani, F., Eltanahy, E., Netzel, M.E., Netzel, G., Lu, Y., Schenk, P.M., Gene expression profiling of astaxanthin and fatty acid pathways in *Haematococcus pluvialis* in response to different LED lighting conditions, *Bioresource Technology* (2017), doi: https://doi.org/10.1016/j.biortech.2017.11.094

Gene expression profiling of astaxanthin and fatty acid pathways in *Haematococcus pluvialis* in response to different LED lighting conditions

Ruijuan Ma[a,b], Skye R. Thomas-Hall[b], Elvis T. Chua[b], Faisal Alsenani[b], Eladl Eltanahy[b,c], Michael E. Netzel[d], Gabriele Netzel[d], Yinghua Lu[a], Peer M. Schenk[b*]

[a]Department of Chemical and Biochemical Engineering, College of Chemistry and Chemical Engineering, Xiamen University, Xiamen 361005, China

[b]Algae Biotechnology Laboratory, School of Agriculture and Food Sciences, The University of Queensland, Brisbane, QLD 4072, Australia

[c]Phycology Laboratory, Botany Department, Faculty of Science, Mansoura University, Egypt

[d]Queensland Alliance for Agriculture and Food Innovation, The University of Queensland, PO Box 156, Archerfield, QLD 4108, Australia

*Corresponding author. E-mail address: p.schenk@uq.edu.au.

Abstract

Haematococcus pluvialis is a green microalga of major interest to industry based on its ability to produce large amounts of astaxanthin. Biosynthesis of astaxanthin and its mono- and di-esters was significantly stimulated under 150 μmol m^{-2} s^{-1} of white LED (W-150) compared with lower light intensities, but the highest astaxanthin amounts were produced under 70 μmol m^{-2} s^{-1} of blue LED (B-70). Transcripts of astaxanthin biosynthesis genes *psy*, *crtO*, and *bkt2* were upregulated under W-150, while *psy*, *lcy*, *crtO*, and *crtR-B* were upregulated by B-70. Total fatty acid content and biosynthesis genes *fata* and all *dgat* genes were induced under W-150, while C18:3n6 biosynthesis and *dgat2a* expression were specifically stimulated by B-70 which was correlated to astaxanthin ester biosynthesis. Nitrogen starvation, various LEDs and the identified upregulated genes may provide useful tools for future metabolic engineering to significantly increase free astaxanthin, its esters and fatty acid precursors in *H. pluvialis*.

Keywords: Astaxanthin esters; fatty acid; gene expression; *Haematococcus pluvialis*; LED lighting conditions.

1. Introduction

Microalgae are phototrophic organisms that convert light energy into chemical energy. Therefore, light is an important factor in the microalgae industry. Compared with traditional fluorescent lamps, light-emitting diodes (LEDs) emit less heat, have longer life-expectancy (Carvalho et al., 2011), and exhibit higher photosynthetically active radiation (PAR) efficiency (Blanken et al., 2013). In addition, due to their small size, LEDs have the advantage for building flexible photobioreactors (Glemser et al., 2016). Because of these, LEDs are rapidly becoming a preferred illumination source for microalgae cultivation. Since different coloured LEDs have distinct wavelengths and energy distributions, the growth rate and metabolite production of microalgae are affected in different ways, and hence various LEDs may offer promising new tools for metabolic engineering by specifically stimulating biosynthesis of desirable compounds (Schuhmann et al., 2014). However, these effects are species-specific. For example, white and green LEDs increased the biomass productivity of *Scenedesmus obliquus* CNW-N and *Scenedesmus obliquus* FSP-3, respectively (Ho et al., 2014), but the growth rates of *Tetraselmis* sp. and *Nannochloropsis* sp. were upregulated under blue LED (Teo et al., 2014). In *Tetraselmis suecica* F&M-M33, red LED induced a high fatty acid content, but carotenoids were not affected by different colored LEDs (Abiusi et al., 2014). Nevertheless, blue LED promoted the carotenoid biosynthesis in *Dunaliella salina* (Fu et al., 2013) and increased the lipid contents of *Tetraselmis* sp. and *Nannochloropsis* sp. (Teo et al., 2014). The reason for this species-dependent effect is still unknown, because there is not much research on the metabolic mechanism of LED regulation like gene expression.

At present, the freshwater green microalga *Haematococcus pluvials* is widely accepted as the best natural resource of astaxanthin, a strong anti-oxidant and red pigment that has broad applications in pharmaceutical, nutraceutical, cosmetic and aquaculture industries (Shah et al.,

2016). For the production of astaxanthin, there are two important physiological stages and cell types in *H. pluvialis*. These are characterized by (1) a fast-growing phase with flagellated vegetative cells that rapidly divide under favourable conditions; (2) an astaxanthin-producing phase where the green vegetative cells transform into palmella, and further change to aplanospores under stress conditions, which is accompanied by astaxanthin accumulation (Fabregas et al., 2001). Many stresses have been shown to induce astaxanthin production, such as nutrient deficiency (Fabregas et al., 1998), high light intensity (Kobayashi et al., 1992), high salinity (Gao et al., 2015), hormone treatment (Gao et al., 2012), and supplementary oxidative stress (Kobayashi et al., 1993). Both, light quality and quantity, have critical roles in astaxanthin accumulation in *H. pluvialis*. LED light has been used for astaxanthin production in *H. pluvialis*, and blue LED light was reported to result in the highest astaxanthin induction (Katsuda et al., 2004; Lababpour et al., 2005). Since more than 95% of astaxanthin in *H. pluvialis* are in ester forms (Holtin et al., 2009; Lorenz & Cysewski, 2000), different LEDs may also affect astaxanthin esters and fatty acid production as well as associated gene expression, which have not been studied. Some articles reported that a higher light intensity of fluorescent lamps induced astaxanthin accumulation and related gene expression (Steinbrenner & Linden, 2003), but the increased heat transfer to microalgae may affect the astaxanthin production and gene expression (Giannelli et al., 2015). Since LEDs generate less heat, the effect of different light intensities on astaxanthin accumulation and gene expression may be different from the effect of fluorescent lamps. In addition, growth rate is affected by light intensity, which leads to a difference of nitrogen consumption rate. This may affect the astaxanthin biosynthesis as well as nitrogen starvation leads to increased fatty acid biosynthesis, the precursors of astaxanthin.

The astaxanthin biosynthesis genes have been identified in *H. pluvialis*, and gene expression has been profiled under salinity stress and hormone treatment (Gao et al., 2015; Gao et al.,

2012). Some fatty acid synthesis genes have been cloned and studied as well (Lei et al., 2012). However, to the authors' knowledge, the expression profile of astaxanthin and fatty acid biosynthesis genes under different LED treatments has not been investigated. It was hypothesized that the gene that catalyses astaxanthin esterification may have an important role in astaxanthin biosynthesis, because most of astaxanthin in *H. pluvialis* is in the ester form. It is reported that diacylglycerol acyltransferase (DGAT) is probably responsible for astaxanthin esterification (Chen et al., 2015). Two DGAT isoforms, DGAT1 and DGAT2, are present in eukaryotes. Noticeably, most algae have been reported to have multiple copies of *DGAT2*, while other eukaryotes have only single copies of *DGAT2* (Chen & Smith, 2012). Nevertheless, the *DGAT* gene family isoforms in *H. pluvialis*, along with their expression profiles under LED treatments have not been studied.

Fatty acid accumulation in microalgae is not a simple case of increased fatty acid biosynthesis. The β-oxidation is a catabolic process by which fatty acid molecules are broken down to generate acetyl-CoA in microalgae. From previous studies, although fatty acid content increased under nitrogen starvation condition, a lack of upregulation of fatty acid biosynthesis genes was observed in *Tetraselmis* sp. M8. Instead, the β-oxidation pathway was downregulated during the early-stationary phase to obtain high fatty acid content (Lim et al., 2017). To the authors' knowledge, there is no study about this metabolic regulation in *H. pluvialis*.

In the current study, the accumulation of astaxanthin and fatty acids in response to different light intensities of white and blue LEDs were investigated. Analysis of the genetic pathways for astaxanthin and fatty acid biosynthesis was performed, as well as *DGAT* and β-oxidation pathway genes. This study will help to understand the effect of different light intensities and different colored LEDs on astaxanthin and fatty acid metabolism of *H. pluvialis*, and also

explain this efficacy at the gene expression level. Moreover, this work will provide a platform for further research on the metabolic regulation of various LEDs in microalgae.

2. Materials and methods

2.1 Algal strain and cultivation conditions

The strain of *H. pluvialis* QLD was isolated from a free-standing water container from the rooftop of the Goddard building (8) at the University of Queensland, St Lucia campus (GPS -27.4977, 153.0120) and maintained in the Algae Biotechnology Laboratory, School of Agriculture and Food Sciences, The University of Queensland, Australia (Gao et al., 2015). Primary stock cultures were grown in 2 L flasks with Bold's Basal medium (BBM) (Ebrahimian et al., 2014), and incubated under 20 μmol m^{-2} s^{-1} white LED light with 16/8 h light/dark cycle at 25°C. The cultures were constantly aerated with filtered air (0.22 μm) until they reached the cell density of 1×10^5 cells mL^{-1}.

The cultures were gently mixed with 1 mM $NaHCO_3$ as carbon source, and then 100 mL, each, was poured to 48 square Petri dishes (130 mm), so that the cells were fully exposed to light. The plates were distributed (12 plates for each light treatment) and exposed to 20 μmol m^{-2} s^{-1} white LED light (W-20), 70 μmol m^{-2} s^{-1} white LED light (W-70), 150 μmol m^{-2} s^{-1} white LED light (W-150) or 70 μmol m^{-2} s^{-1} blue LED light (B-70). In order to have nitrogen depleted at the same time, after 2-day incubated over each light treatment, the cultures were harvested by centrifugation at 3500xg for 10 min, washed once with fresh nitrate-free BBM medium (BBM-N), and then resuspended in BBM-N medium. Cell densities were adjusted to 2×10^5 cells mL^{-1}, and then the cultures were poured back to square Petri dishes and exposed to the same light conditions for another 6 days. For the control experiment without changing nitrogen, the plates were distributed and exposed to W-20, W-70, and W-150 for 5 days.

Light intensity and spectral photon distribution were measured with an HR-350 LED meter (HiPoint). Nitrate levels were detected using API Nutrient testing kits as reported previously (Adarme-Vega et al., 2014). Cells were counted using a Neubauer haemocytometer. Samples for RNA extraction, astaxanthin and fatty acid analyses were collected on day 0, 2, 5, and 8 in the experiment with the nitrogen control, and on day 0, 2, and 5 in the experiment without the nitrogen control. At each sampling time, the collected cultures from four plates were mixed as one sample. Samples of 15 mL, each, were harvested by centrifugation, washed with phosphate buffered saline (PBS), immediately frozen by liquid nitrogen and then stored at -80°C until RNA extraction was performed. Samples of 65 mL, each, were harvested by centrifugation, washed with distilled water, and then lyophilized for astaxanthin and fatty acid analyses.

2.2 Astaxanthin extraction and analysis

About 10 mg of dry biomass was mixed with 0.5 g glass beads and vortexed for 2 min. Then 5 mL dichloromethane/methanol (1:1, v/v) was added and vortexed for 1 min. The mixture was centrifuged at 3000×g for 3 min, and the supernatant was collected. The pellet was extracted repeatedly with 3 mL dichloromethane/methanol (1:1, v/v) until it became colorless. The collected pigment extract was dried under nitrogen gas, and then redissolved with 2 mL of acetonitrile/methanol (3:1) and used for quantification of carotenoids. Apo-8-β-carotenal was used as an internal standard.

Separation and identification of carotenoids were carried out on an Acquity UPLC system (Waters, Milford, MA, USA) equipped with a photodiode array (PDA) detector. Samples (5.0 μL) were injected into an Acquity UPLC Shield C18 BEH column (2.1×100 mm, 1.7 μm particle size; Waters). The analysis method is based on (Mulders et al., 2015; Weesepoel et al., 2013) with some modifications. The eluents were: (A) 50% (v/v) acetonitrile in

demineralized water, (B) acetonitrile, and (C) ethyl acetate. All eluents contained 0.1% (v/v) formic acid. The flow rate was maintained at 300 μL min^{-1}. The program was initiated from 30% A/70% B and then as follows: to 10 min-linear gradient to 100% B, to 15 min-isocratic at 100% B, to 20 min-linear gradient to 87.5% B/12.5% C, to 21 min-linear gradient to 70% B/30% C, to 28 min-linear gradient to 100% C and to 29 min-isocratic at 100% C. After 29 min, the eluent composition reverted to its initial composition in 1 min followed by an equilibration phase of 12 min. The detection wavelength for the PDA detector was adjusted to 460 nm.

2.3 Fatty acid methyl ester (FAME) analysis

About 10 mg dry algae in 8 mL vials were mixed with 100 μL of recovery standard heneicosanoic acid (1.2 mg mL^{-1}) and 2 mL 5% acetyl chloride in methanol. The vials were then heated in a 90°C waterbath for 1 h. After the samples were cooled to room temperature, 2 mL of 0.9% sodium chloride solution and 2 mL of hexane were added. The mixture was then vortexed and centrifuged at 400×g for 5 min. 1 mL hexane phase was collected and added with 100 μL of internal standard methyl heptadecanoic acid (1 mg mL^{-1}) dissolved in heptane.

Qualification and quantification analysis of FAMEs were performed on a GCMS-QP2010 ULTRA (Shimadzu, Kyoto, Japan), which was equipped with a Stabilwax® (Crossbond® Carbowax® polyethylene glycol) capillary column (30 m × 0.25 mm ID × 0.5 μm; Restek, Bellefonte, PA, USA). Helium was used as a carrier gas at a constant linear velocity of 42.7 cm/s. The temperature of the injection port was set at 250°C. Samples of 1 μL, each, were injected in split mode with a split ratio of 10. The mass spectrometer was operated with the ion source and interface temperatures at 200°C and 250°C, respectively. The mass range scanned was from 40 to 500 m z^{-1}. The oven temperature program was as follows: initial

temperature maintained at 70°C for 2 min, increased to 180°C at a rate of 30°C/min, followed by a rate of 4°C/min to 220°C and held for 5 min, 10°C/min to 250°C and held for 9.35 min. The fatty acids were identified with a Supelco® 37-component FAME mix standard (Sigma-Aldrich, St. Louis, MO, USA) and verified using the NIST14 library.

2.4 RNA isolation and real-time quantitative reverse transcriptase PCR

RNA was isolated according to an extraction procedure reported previously (Cazzonelli et al., 1998) with the following modification. Frozen samples in 1.5 mL Eppendorf tubes were mixed with 400 μL lysis buffer (150 mM pH 7.5 Tris, 2% (w/v) SDS, 50 mM EDTA, 1% (v/v) β-mercaptoethanol), and vortexed for 2 min at room temperature. A total of 100 μL absolute ethanol was added and samples were vortexed for 1 min, followed by the addition of 44 μL 5 M potassium acetate, and then vortexing for 1 min. A total of 500 μL chloroform: isoamyl alcohol (24:1) was added to the homogenate, vortexed for another 1 min, and then centrifuged at 16000×g for 3 min. The recovered aqueous phase was removed to a new tube and extracted with 500 μL phenol: chloroform: isoamyl alcohol (25:24:1). About 400 μL of the aqueous phase was removed to a new tube and mixed with 1 mL absolute ethanol. After vortexing for 1 min, the mixture was incubated at -80°C for 10 min for precipitation, and then centrifuged for 5 min at 16000×g (4°C). The pellet was washed with 80% ethanol, resuspended in 75 μL diethyl pyrocarbonate (DEPC)-treated water, and mixed with 25 μL 8 M DEPC LiCl. After 2 h of incubation at 4°C, the RNA was collected by centrifugation at 16000×g for 3 min (4°C). The pellet was washed with 80% ethanol and vacuum-dried. Purified RNA was resuspended in 50 μL DEPC-treated H_2O, and then incubated with DNase I (New England Biolabs) to remove DNA contamination.

First-strand complementary DNA (cDNA) synthesis was performed by a Tetro cDNA Synthesis Kit (Bioline) according to the manufacturer's instructions. A total of 2.5 μg of total

RNA in a 20 μL reaction was synthesized to cDNA using both random hexamers and oligo dT primers. Specific primers of astaxanthin and fatty acid biosynthesis genes have been described previously (Gao et al., 2015; Lei et al., 2012). Specific primers of *dgat* genes and fatty acid degradation pathway genes were designed by the primer BLAST tool from the NCBI website (http://www.ncbi.nlm.nih.gov/tools/primer-blast/).

Real-time quantitative reverse transcriptase PCR (qRT-PCR) assays were performed in a 10 μL reaction containing 5 μL SYBR® Green PCR Master Mix, 1 μL of a primer mix (forward and reverse, 3 μM each), and 4 μL of cDNA templates (10 ng μL^{-1}). Reagent and cDNA were dispensed by a pipetting robot (Eppendorf epMotion 5075, Eppendorf) to 384 well-plates. The qRT-PCR was performed on ViiA 7 Real-Time PCR System (Applied Biosystems). The program was set as follows: stage 1, 95°C for 10 min; stage 2, 40 cycles of 95°C for 15 s and 60°C for 1 min; stage 3, 1 cycle of 95°C for 15 s, 60°C for 1 min and 95°C for 15 s. Relative expression of each target gene was investigated using three biological replicates with two technical replicates, each. Transcript levels were normalized to *actin* gene, as it has been used in other studies (Eom et al., 2006; Lei et al., 2012). PCR efficiency for each sample was determined by the LinRegPCR program, and primer efficiency (PE) was calculated by the mean of efficiency values obtained from the individual samples (Nymark et al., 2009; Ramakers et al., 2003). The formula for gene expression calculation is:

$$Relative\ expression\ ratio = \frac{\mathrm{PE}gene^{-\mathrm{Ct}\,gene}}{\mathrm{PE}actin^{-\mathrm{Ct}\,actin}}.$$

2.5 Statistical analysis

The experiments were conducted with biological triplicates from separate microalgal cultures in this study. Data in the figure are shown as average of triplicates and error bars are standard errors. For all data analyses, two-tailed t-tests were performed, and *P* values <0.05 were considered statistically significant.

3. Results and discussion

3.1 Growth characteristics and residual nitrate

H. pluvialis was subjected to growth under various LEDs. In the control experiment without changing nitrogen, high light intensity of white LED (W-70 and W-150) increased cell growth and nitrate consumption. Nitrate was depleted in the media under W-70 and W-150 on day 3, but still replete under W-20. Since nitrogen is an important factor of astaxanthin biosynthesis, the various nitrate consumption rates may interfere in the study of the effect of different LEDs on *H. pluvialis*. Therefore, the algal cultures were centrifuged and resuspended with BBM-N medium on day 2 to have nitrogen depleted at the same time.

Cell growth characteristics and residual nitrate contents in the media are shown in Fig. 1A and B, respectively. Nitrate concentration decreased but was still replete from day 0 to 2. W-150 displayed the fastest nitrate consumption. Residual nitrate was not significantly different under W-70 and B-70, and the consumption was lowest for W-20. From day 0 to 2, cell numbers increased in the order B-70>W-150>W-70>W-20. After nitrate was depleted, cell numbers still increased from day 2 to 3, and was highest for W-70. This could be due to nitrate still stored in the cells during this short time. Cell numbers levelled for B-70 from day 4 to 8, but decreased under W-20, W-70 and W-150 on day 4, then levelled from day 5 to 8. From day 4 to 8, cell numbers under W-70 and B-70 were higher than W-150 and W-20. The cell number of W-150 was highest when nitrate was replete, but at lower levels after nitrate was depleted, so *H. pluvialis* cells may have been damaged under high light conditions (W-150) after nitrate was depleted.

3.2 Astaxanthin content under different LED lighting conditions

In *H. pluvialis*, astaxanthin is predominantly esterified with fatty acids, thus three forms of astaxanthin are present: free astaxanthin, astaxanthin monoesters (ME) and diesters (DE) (Miao et al., 2006). It was reported that nitrogen starvation, high light intensity, and blue light induced astaxanthin production (Katsuda et al., 2004; Scibilia et al., 2015), but the effect between nitrogen and light as well as the composition of each astaxanthin that form under these conditions have not been studied.

As shown in Fig. 1, free astaxanthin content was 0.17 mg g^{-1} on day 0, then decreased to 0.07, 0.12, 0.15 mg g^{-1} under W-20, W-70, and W-150, respectively, on day 2. However, this value increased to 0.22 mg g^{-1} for B-70 on day 2 when the nitrogen was replete. After nitrogen was depleted, free astaxanthin content for W-20 increased to 0.17 mg g^{-1} on day 5, and then decreased to 0.11 mg g^{-1} on day 8. For W-70, free astaxanthin content was at the same level on day 5, and then decreased to 0.07 mg g^{-1} on day 8. Free astaxanthin content under W-150 and B-70 continuously decreased to 0.07 and 0.04 mg g^{-1}, respectively, on day 5, 0.18 and 0.09 mg g^{-1} on day 8, respectively. It is worth noting that the free astaxanthin content increased in the order W-150>W-70>W-20 when nitrogen was replete (on day 2), but the trend was W-150<W-70<W-20 when nitrogen was depleted (on day 5 and 8). However, compared with W-70 and W-150, free astaxanthin was higher for B-70 independent of the nitrogen concentration (Fig. 1C).

Astaxanthin ME is the major form of astaxanthin in *H. pluvialis*. The astaxanthin ME content was 1.24 mg g^{-1} on day 0. When nitrogen was replete, it remained at the same level for W-20, W-70 and B-70, but increased to 2.89 mg g^{-1} for W-150 on day 2. After nitrogen was depleted, astaxanthin ME content continuously increased for all light conditions on both days, 5 and 8. On day 5, it was higher under W-150 than W-70 and W-20, but similar for B-70 and W-150. Interestingly, B-70 induced the highest astaxanthin ME on day 8. The contents were similar under W-150 and W-70, but higher than W-20 (Fig. 1D).

Astaxanthin DE was not detected on day 0 and 2 for W-20 and W-70. By contrast, W-150 (0.08 mg g^{-1}) and B-70 (0.09 mg g^{-1}) had higher astaxanthin DE contents on day 2. After nitrogen was depleted, astaxanthin DE content increased drastically. On both days, 5 and 8, astaxanthin DE content was highest for B-70 (Fig. 1E). Astaxanthin DE content reached 1.45 mg g^{-1} under B-70 on day 8, which was 2.74, 2.07, and 1.64 fold of W-20, W-70, and W-150, respectively.

Since astaxanthin is predominantly in ester form in *H. pluvialis*, total astaxanthin content had a similar trend as astaxanthin ME and DE. The total astaxanthin contents did not change under W-20, W-70, and B-70 from day 0 to day 2, but were significantly upregulated in W-150. Astaxanthin continuously increased for all light conditions from day 2 to day 8. The total astaxanthin content increased in the order B-70>W-150>W-70>W-20 on day 5. B-70 induced the highest amount of total astaxanthin (21.45 mg g^{-1}) on day 8, which was 2.99-, 1.59-, and 1.47-fold of W-20, W-70, and W-150, respectively. The total astaxanthin contents were similar for W-70 and W-150, but higher than W-20 on day 8 (Fig. 1F).

3.3 Fatty acid content under different LED lighting conditions

Fig. 2 shows the fatty acid profiles under different LED treatments on different days. The major fatty acid components are palmitic acid (C16:0), stearic acid (C18:0), oleic acid (C18:1n9), linoleic acid (C18:2n6), α-linolenic acid (C18:3n3), γ-linolenic acid (C18:3n6), and arachidonic acid (C20:4n6). They are the main fatty acids in astaxanthin esters (Weesepoel et al., 2013) and hence their profiling in response to various LED lighting conditions was considered important.

The contents of C16:0, C18:0, C18:1n9 and C18:2n6 were significantly increased from day 2 to day 8 for all light conditions, mostly increasing in the ranking of W-150>W-70>W-20. C16:0 and C18:0 contents of B-70 were similar to W-70 and W-150, but higher than W-20

from day 2 to day 8. C18:1n9 and C18:2n6 contents were the lowest for B-70 on day 2. C18:1n9 content was higher under B-70 than W-20 and W-70, but W-150 obtained the highest content on day 5. On day 8, the C18:1n9 content was similar under B-70 and W-70 on day 8. There was no significant difference of C18:2n6 content between B-70 and W-70 on day 5 and day 8.

C18:3n3 and C18:3n6 contents kept at relatively stable levels from day 0 to day 8. C18:3n6 content was similar under W-70, W-150, and B-70, but slightly lower for W-20. Noticeably, C18:3n3 content was significantly higher for B-70 on day 2 and 8. C20:4n6 content did not change on day 2, but slightly decreased from day 2 to 8. Its content was higher for W-20 on day 5 and 8.

Saturated fatty acid (SFA), monounsaturated fatty acid (MUFA), polyunsaturated fatty acid (PUFA) and total fatty acid (TFA) did not significantly change from day 0 to 2, and then continuously increased from day 2 to day 8. This trend is similar to the increasing levels of astaxanthin esters. On day 2, PUFA and TFA contents were slightly higher for W-150 and B-70. On day 5, SFA, MUFA, PUFA, and TFA content were increasing in the order W-150>W-70>W-20. There were no significant differences in SFA, PUFA, and TFA levels between B-70 and W-150 which were higher than W-20 and W-70, while MUFA content for B-70 was between W-70 and W-150 on day 5. On day 8, SFA, PUFA, and TFA contents were higher under W-70, W-150, and B-70 compared with W-20, but there were no significant differences among these three light conditions. MUFA content was higher for W-150 than W-70 and B-70, but lower for W-20 on day 8.

Both, total astaxanthin and total fatty acid contents, were higher for W-150 than for W-70 and W-20 on day 5, while their contents were similar for W-150 and W-70 on day 8, which were higher than W-20. These results were consistent with previous studies claiming that

astaxanthin biosynthesis was coordinated with fatty acid biosynthesis for high light conditions (Chen et al., 2015; Zhekisheva et al., 2002). However, although B-70 induced a higher amount of total astaxanthin than W-150, especially astaxanthin esters, the total fatty acid content for B-70 was not quite as high as W-150. Nevertheless, C18:3n3 composition for B-70 was significantly higher than W-150. Since C18:3 astaxanthin ME is one of the main astaxanthin esters in *H. pluvialis* (Miao et al., 2006), increased production of C18:3n3 is likely linked to the increased production astaxanthin ME observed for the B-70 treatment.

3.4 Transcript expression of carotenogenic genes

The transcript level of carotenogenic genes varied between each treatment. Isopentenyl pyrophosphate isomerase (IPI) catalyzes the isomerization of IPP (isopentenyl diphosphate) to DMAPP (dimethylallyl diphosphate), which are the precursors of the carotenoid backbone (Lee & Schmidt-Dannert, 2002). The transcript levels of *ipi* 1 and *ipi* 2 were unchanged for W-20 on day 2 compared with day 0, but decreased under W-150, W-70, and B-70. After nitrogen deprivation (day 5 and day 8), *ipi* 1 and *ipi* 2 expression dropped under W-20 as well. In the control experiment of without changing nitrogen, W-20 was still nitrogen-replete on day 5. Consistently, the gene expressions of *ipi* 1 and *ipi* 2 were higher for W-20 than W-70 and W-150. These results suggest that both, high light intensity of white LED and nitrogen starvation, downregulate *ipi* 1 and *ipi* 2 expressions.

Phytoene synthase (PSY) is a key enzyme for carotenoid biosynthesis, committing a rate-limiting step (Gong & Bassi, 2016). No changes were observed in the gene expression of *psy* on day 2 under W-20, W-70, and B-70. On the other hand, a slight increase was observed for W-150. Transcript abundance for *psy* was significantly higher for B-70 on day 5. On day 8, *psy* expression significantly increased for all light conditions, and its expression was higher for both W-150 and B-70.

Lycopene β-cyclase (LCY) catalyzes the flux from lycopene to β-carotene. The expression of *lcy* slightly increased on day 2 for all light treatment. On day 5, *lcy* expression decreased for W-70 and W-150, but did not change for W-20 and B-70. However, it was significantly upregulated on day 8 for all conditions. Compared with W-20 and W-70, *lcy* expression was lower for W-150, but significantly higher for B-70. However, W-150 upregulated *lcy* expression on day 4 and 5 in the control experiment without changing nitrogen. Since nitrogen was depleted for W-150 but still replete for W-20 at this time, nitrogen depletion could have caused the increased expression of *lcy* under W-150. Therefore, *lcy* expression was upregulated by nitrogen starvation but not high light intensity.

CRTO and BKT2 are two types of β-carotene ketolases/oxygenases that, together with CRTR-B (β-carotene hydroxylase), catalyze β-carotene to astaxanthin. The expression of *bkt2* was similar on day 0 and 2, and then continuously increased from day 2 to day 8. A significant increase in *bkt2* expression was observed for W-150 from day 5 to day 8. On the other hand, *crtO* and *crtR-B* transcripts were low when nitrogen was replete (day 0 and 2), but these genes were significantly upregulated for all light treatments after nitrogen was depleted (day 5 and 8). B-70 significantly upregulated *crtO* and *crtR-B* expressions on day 5, while W-150 induced *crtO* on day 8, but did not change *crtR-B* expression on either day 5 or day 8. By contrast, W-150 significantly upregulated *crtR-B* expression on day 4 and 5 in the control experiment without changing nitrogen. This upregulation may be due to nitrogen depletion at this time point. Thus, *crtR-B* expression was upregulated by nitrogen starvation but not high light intensity.

It is worth noting that B-70 upregulated the expressions of *psy*, *lcy*, *crtO*, and *crtR-B*, while W-150 upregulated the expressions of *psy*, *crtO*, and *bkt2* after nitrogen was depleted. From the astaxanthin measurement results, it can be observed that B-70 and W-150 increased total astaxanthin contents compared with both W-20 and W-70. Therefore, the increase of

astaxanthin contents under blue LED and high intensity white LED occur via the upregulation of distinct genes. To the authors' knowledge, this is the first investigation on gene expression of astaxanthin biosynthesis pathway under different LED lighting conditions. The manipulation of LEDs may provide useful tools to stimulate cellular astaxanthin biosynthesis for scientific and industrial purposes.

3.5 Transcript expression of fatty acid biosynthesis genes

The mRNA expressions of all fatty acid biosynthesis genes were low when nitrogen was replete (day 0 and 2), but were significantly upregulated after nitrogen was depleted (day 5 and 8) for all light treatments (Fig. 4). Biotin carboxylase (BC) is a subunit of acetyl coenzyme A carboxylase biotin carboxylase. It catalyzes the first rate-limiting step of fatty acid biosynthesis from acetyl-CoA to malonyl-CoA. The expression of *bc* was similar under W-20, W-70, and W-150 on day 5, but significantly upregulated for B-70. The same trend was observed on day 8.

Acyl carrier protein (ACP) acts as an important component in both fatty acid and polyketide biosynthesis, where a growing chain is bound to a thiol ester at the distal thiol of a 4'-phosphopantetheine moiety. The expression of *acp* was higher for W-20 and B-70 than W-70 and W-150 on day 2. On day 5 and 8, *acp* expression was similar under W-20, W-70, and W-150, but significantly upregulated under B-70.

Malonyl-CoA:ACP transacylase (MCTK) transfers malonyl moiety from malonyl-CoA onto the acyl carrier protein, which extends the length of the growing acyl chain by two carbons in fatty acid elongation step. After that, the 3-ketoacyl-ACP synthase (KAS) catalyses the condensation reaction between acetyl CoA and malonyl ACP. The *mctk* and *kas* expressions were higher under W-20 and B-70 than W-70 and W-150 on either day 5 or day 8.

Acyl-ACP thioesterase (FATA) is the chain-length-determining enzyme in fatty acid biosynthesis, catalysing the hydrolysis of the thioester bond of acyl-ACP to release free fatty acid and ACP. The *fata* expression level was higher under W-150 than W-20 and W-70, and B-70 induced the highest expression of *fata* on day 5.

Based on the above results, it can be concluded that both W-150 and B-70 upregulated *fata* expression on day 5, which is consistent with the increased levels of SFA, MUFA and TFA contents on day 5. In addition, B-70 upregulated *bc*, *acp*, *mctk*, and *kas* on both day 5 and 8. However, W-150 downregulated *mctk* and *kas*. But C16:0, C18:0, and C18:2n6 contents were significantly increased under W-150. To the authors' knowledge, the genes responsible for synthesis of these fatty acids are still unidentified in *H. pluvialis*. Hence, the increase of these fatty acid levels may be a result of upregulation of these genes rather than *mctk* and *kas*.

Stearoyl-ACP-desaturase (SAD) catalyzes the conversion of 18:0 to C18:1n9, which is important in determining the ratio of saturated to unsaturated fatty acids (Zhao et al., 2015). The expression of *sad* was significantly upregulated on day 5 and 8 (nitrogen depleted) in all treatments, which was consistent with the increase of C18:1n9. This was similar to the control experiment without changing nitrogen where *sad* expression was upregulated under W-150 and W-70 on day 3, 4, and 5 when nitrogen was depleted. However, in the experiment with nitrogen, increasing *sad* expression did not directly correlate with the measured amounts of C18:1n9 for the different treatments. It is known that there are many *sad* genes in plants (Kachroo et al., 2007; Parvini et al., 2016), which may also exist in green algae but these have not yet been studied. The increase of C18:1n9 under W-150 may be a result of upregulation of the expression of the other *sad* genes. Alternatively, the high accumulation of C18:1n9 in the W-150 treatment may have been due to regulation from other pathways, i.e. lipid catabolism.

The ω-3 fatty acid desaturase (FAD) catalyzes the conversion of C18:2n6 to C18:3n3; its encoding gene was significantly upregulated in all treatments with nitrogen depletion. Compared with W-20, W-70, and B-70, *fad* expression was significantly upregulated by W-150 on day 5 and 8. However, although C18:3n3 content was highest for B-70, *fad* expression was not specifically upregulated by B-70. Three *fad* genes have been identified in plants, and their expression levels are different (Bilyeu et al., 2003). Although a study described that only one *fad* gene was discovered in *Chlamydomonas reinhardtii* (Nguyen et al., 2013), three distinct *Chlamydomonas fad* genes were identified in Genebank (KC012989.1, GQ888689.1, EF110555.1). In *H. pluvialis*, various homologs of this gene may exist, and the induction of C18:3n3 may be due to upregulation of another *fad* gene. Alternatively, as previously stated, C18:3 astaxanthin ME is one of the major esters in *H. pluvialis* (Miao et al., 2006). The increase of C18:3n3 content under B-70 may have been due to the increased flux to C18:3n3 astaxanthin ester, which can lock away the C18:3n3 and allow it to build up, rather than induction of C18:3n3 biosynthesis by FAD. However, the upregulation of *fad* expression under W-150 did not lead to the increase of C18:3n3 content. This may be because fatty acid degradation was increased.

3.6 Transcript expression of diacylglycerol acyltransferase genes

Diacylglycerol acyltransferase (DGAT) catalyzes the last critical step of the triacylglycerol (TAG) biosynthesis pathway, which is the rate-limiting step for lipid accumulation (Lung & Weselake, 2006). On the other hand, it has been reported that DGAT probably also catalyzes astaxanthin esterification (Chen et al., 2015). Two types of DGATs (DGAT1 and DGAT2) have been identified in some algae, and multiple isoforms of *DGAT2* were uniquely found (Chen & Smith, 2012). By comparing to DGAT sequences of *Chlamydomonas reinhardtii*, one homolog sequence of DGAT1 and four isoforms of DGAT2 were identified from the *Haematococcus* transcriptome database (SRX384371).

Expression of *dgat1* was low level on day 2, and then upregulated on day 5 and 8. On day 5, *dgat1* expression was significantly higher under W-150. Its expression was similar under W-70 and B-70, while W-20 showed the lowest *dgat1* expression (Fig. 5A). This increasing expression trend corresponds to the total fatty acid contents measured (Fig. 2).

The transcript abundance of four members of the *dgat2* family is shown in Fig. 5B. Expression of *dgat2a* and *dgat2b* did not change on day 0 and 2, but increased on day 5 and 8. The transcript level of *dgat2a* was slightly higher under B-70 than W-150 and W-70, and W-20 displayed the lowest *dgat2a* expression on day 8, which is consistent with astaxanthin ester contents measured (Fig. 1). The *dgat2b* expression was slightly higher under W-150 on day 8, while *dgat2d* and *dgat2e* transcripts were decreased on day 2, but increased on day 5 and 8. Expression of *dgat2d* was upregulated by W-150 and B-70, compared with W-20 and W-70 on day 5. Expression of *dgat2e* was slightly upregulated by W-150 on day 5.

From the above results, it can be concluded that all *H. pluvialis dgat* genes were upregulated after nitrogen was depleted (day 5 and 8), which was consistent with the increase of total fatty acid and astaxanthin esters. Expression of *dgat1* was upregulated by W-150 which is consistent with total fatty acid accumulation. And the upregulation of *dgat2a*, *dgat2b*, *dgat2d*, and *dgat2e* expression by W-150 may further assist to increase total fatty acid. Expression of *dgat2a* was also induced by blue LED which was coincided with the measured increase of astaxanthin esters, and is likely to have contributed to the increase of astaxanthin esters. This result is consistent with a previous study that suggested that DGAT may catalyze astaxanthin esterification (Chen et al., 2015). The present study identifies distinct DGAT isoforms and profiles their expression under different LED lighting conditions. The results may help to better understand the DGAT functions in fatty acid biosynthesis and astaxanthin esterification.

3.7 Transcript expression of fatty acid degradation genes

By comparing to the gene sequences of *Chlamydomonas reinhardtii*, *Chlorella variabilis*, *Volvox carteri* f. *nagariensis*, *Helicosporidium* sp. and *Tetraselmis* sp., six fatty acid degradation genes were identified from the *Haematococcus* transcriptome database (SRX384371). Transcript profiling of fatty acid degradation pathway genes is shown in Fig. 6.

Triacylglycerol lipase (TAGL) catalyzes the conversion of triacylglycerol to diacylglycerol and free fatty acid. The expression of *tagl* was unchanged on day 2 and 5, but significantly upregulated on day 8 under W-70, W-150, and B-70, which were 3.83-, 5.91-, and 3.57-fold, respectively, of W-20. The upregulation of *tagl* followed a similar profile to the total fatty acid accumulation of the different treatments, suggesting the expression of this gene is correlated with the total lipid content in the cells.

Long chain fatty acyl-CoA synthetase (LACS) is an enzyme of the ligase family that activates the breakdown of complex fatty acids, which channels fatty acids into β-oxidation. The expression of *lacs* did not change under W-20, but was downregulated under W-70, W-150, and B-70 on day 2, and then upregulated on day 5 and 8. The transcript of *lacs* was higher under W-150 than W-20, W-70, and B-70 on day 5 and 8. Acyl-CoA oxidase (ACO), enoyl-CoA hydratase (ECH), hydroxyacyl-CoA dehydrogenase (HAD) and ketoacyl-CoA thiolase (KAT) are responsible for β-oxidation of fatty acids. All four genes were downregulated under W-70, W-150, and B-70 on day 2 (nitrogen replete), but upregulated at all light treatments on day 5 and 8 (nitrogen depleted). The upregulation of β-oxidation pathway genes after nitrogen depletion is consistent with the previous study in *Tetraselmis* sp. M8, that the expression of these genes increased under 3 days' nitrogen starvation treatment as algae may need to access energy reserves (Lim et al., 2017).

The *fad* expression under W-150 was upregulated on day 5 and 8, but C18:3n3 content was not increased on these days. Noticeably, the β-oxidation genes were upregulated for W-150

on day 5 and 8. The reason that C18:3n3 content did not increase may be the upregulation of fatty acid degradation. However, the gene responsible for C18:3n3 degradation has not been identified in *H. pluvialis*. This metabolic regulation still needs to be further studied.

4. Conclusions

Nitrogen starvation induced total astaxanthin and fatty acid content, along with associated gene expressions (except for *ipi1* and *ipi2*). W-150 and B-70 significantly increased astaxanthin content in *H. pluvialis*. However, these two conditions upregulated distinct gene expressions of the astaxanthin biosynthesis pathway. Fatty acid content was increased by W-150, and *fata* and all *dgat* genes were upregulated. The expression of *dgat2a* was upregulated by B-70 and may be correlated to the production of astaxanthin esters. The upregulation of fatty acid degradation pathway genes at late time points after nitrogen depletion is consistent with a previous study in *Tetraselmis* sp. M8.

Acknowledgements

RM was funded by China Scholarship Council.

Appendix A. Supplementary data

Supplementary data associated with this article can be found in the online version.

References

1. Abiusi, F., Sampietro, G., Marturano, G., Biondi, N., Rodolfi, L., D'Ottavio, M., Tredici, M.R., 2014. Growth, photosynthetic efficiency, and biochemical composition of *Tetraselmis suecica* F&M-M33 grown with LEDs of different colors. Biotechnol Bioeng. 111(5), 956-964.
2. Adarme-Vega, T.C., Thomas-Hall, S.R., Lim, D.K.Y., Schenk, P.M., 2014. Effects of long chain fatty acid synthesis and associated gene expression in microalga *Tetraselmis* sp. Mar Drugs. 12(6), 3381-3398.
3. Bilyeu, K.D., Palavalli, L., Sleper, D.A., Beuselinck, P.R., 2003. Three microsomal omega-3 fatty-acid desaturase genes contribute to soybean linolenic acid levels. Crop Sci 43(5), 1833-1838.
4. Blanken, W., Cuaresma, M., Wijffels, R.H., Janssen, M., 2013. Cultivation of microalgae on artificial light comes at a cost. Algal Res. 2(4), 333-340.
5. Carvalho, A.P., Silva, S.O., Baptista, J.M., Malcata, F.X., 2011. Light requirements in microalgal photobioreactors: an overview of biophotonic aspects. Appl Microbiol Biot. 89(5), 1275-1288.
6. Cazzonelli, C.I., Cavallaro, A.S., Botella, J.R., 1998. Cloning and characterisation of ripening-induced ethylene biosynthetic genes from non-climacteric pineapple (*Ananas comosus*) fruits. Aust J Plant Physiol. 25(5), 513-518.
7. Chen, G.Q., Wang, B.B., Han, D.X., Sommerfeld, M., Lu, Y.H., Chen, F., Hu, Q., 2015. Molecular mechanisms of the coordination between astaxanthin and fatty acid biosynthesis in *Haematococcus pluvialis* (Chlorophyceae). Plant J. 81(1), 95-107.
8. Chen, J.E., Smith, A.G., 2012. A look at diacylglycerol acyltransferases (DGATs) in algae. J Biotechnol. 162(1), 28-39.
9. Ebrahimian, A., Kariminia, H.R., Vosoughi, M., 2014. Lipid production in mixotrophic cultivation of *Chlorella vulgaris* in a mixture of primary and secondary municipal wastewater. Renew Energ. 71, 502-508.
10. Eom, H., Lee, C.G., Jin, E., 2006. Gene expression profile analysis in astaxanthin-induced *Haematococcus pluvialis* using a cDNA microarray. Planta. 223(6), 1231-1242.
11. Fabregas, J., Dominguez, A., Alvarez, D.G., Lamela, T., Otero, A., 1998. Induction of astaxanthin accumulation by nitrogen and magnesium deficiencies in *Haematococcus pluvialis*. Biotechnol Lett. 20(6), 623-626.
12. Fabregas, J., Otero, A., Maseda, A., Dominguez, A., 2001. Two-stage cultures for the production of Astaxanthin from *Haematococcus pluvialis*. J Biotechnol. 89(1), 65-71.
13. Fu, W.Q., Guomundsson, O., Paglia, G., Herjolfsson, G., Andresson, O.S., Palsson, B.O., Brynjolfsson, S., 2013. Enhancement of carotenoid biosynthesis in the green microalga *Dunaliella salina* with light-emitting diodes and adaptive laboratory evolution. Appl Microbiol Biot. 97(6), 2395-2403.
14. Gao, Z.Q., Meng, C.X., Chen, Y.C., Ahmed, F., Mangott, A., Schenk, P.M., Li, Y., 2015. Comparison of astaxanthin accumulation and biosynthesis gene expression of three *Haematococcus pluvialis* strains upon salinity stress. J Appl Phycol. 27(5), 1853-1860.
15. Gao, Z.Q., Meng, C.X., Zhang, X.W., Xu, D., Miao, X.X., Wang, Y.T., Yang, L.M., Lv, H.X., Chen, L.L., Ye, N.H., 2012. Induction of salicylic acid (SA) on transcriptional expression of eight carotenoid genes and astaxanthin accumulation in *Haematococcus pluvialis*. Enzyme Microb Tech. 51(4), 225-230.
16. Giannelli, L., Yamada, H., Katsuda, T., Yamaji, H., 2015. Effects of temperature on the astaxanthin productivity and light harvesting characteristics of the green alga *Haematococcus pluvialis*. J Biosci Bioeng. 119(3), 345-350.
17. Glemser, M., Heining, M., Schmidt, J., Becker, A., Garbe, D., Buchholz, R., Bruck, T., 2016. Application of light-emitting diodes (LEDs) in cultivation of phototrophic microalgae: current state and perspectives. Appl Microbiol Biot. 100(3), 1077-1088.
18. Gong, M.Y., Bassi, A., 2016. Carotenoids from microalgae: A review of recent developments. Biotechnol Adv. 34(8), 1396-1412.
19. Ho, S.H., Chan, M.C., Liu, C.C., Chen, C.Y., Lee, W.L., Lee, D.J., Chang, J.S., 2014. Enhancing lutein productivity of an indigenous microalga *Scenedesmus obliquus* FSP-3 using light-related strategies. Bioresour Technol. 152, 275-282.
20. Holtin, K., Kuehnle, M., Rehbein, J., Schuler, P., Nicholson, G., Albert, K., 2009. Determination of astaxanthin and astaxanthin esters in the microalgae *Haematococcus pluvialis* by LC-

(APCI)MS and characterization of predominant carotenoid isomers by NMR spectroscopy. Anal Bioanal Chem. 395(6), 1613-1622.
21. Kachroo, A., Shanklin, J., Whittle, E., Lapchyk, L., Hildebrand, D., Kachroo, P., 2007. The *Arabidopsis* stearoyl-acyl carrier protein-desaturase family and the contribution of leaf isoforms to oleic acid synthesis. Plant Mol Biol. 63(2), 257-271.
22. Katsuda, T., Lababpour, A., Shimahara, K., Katoh, S., 2004. Astaxanthin production by *Haematococcus pluvialis* under illumination with LEDs. Enzyme Microb Tech. 35(1), 81-86.
23. Kobayashi, M., Kakizono, T., Nagai, S., 1993. Enhanced carotenoid biosynthesis by oxidative stress in acetate-induced cyst cells of a green unicellular alga, *Haematococcus pluvialis*. Appl Environ Microb. 59(3), 867-873.
24. Kobayashi, M., Kakizono, T., Nishio, N., Nagai, S., 1992. Effects of light intensity, light quality, and illumination cycle on astaxanthin formation in a green alga, *Haematococcus pluvialis*. J Ferment Bioeng. 74(1), 61-63.
25. Lababpour, A., Shimahara, K., Hada, K., Kyoui, Y., Katsuda, T., Katoh, S., 2005. Fed-batch culture under illumination with blue light emitting diodes (LEDs) for astaxanthin production by *Haematococcus pluvialis*. J Biosci Bioeng. 100(3), 339-342.
26. Lee, P.C., Schmidt-Dannert, C., 2002. Metabolic engineering towards biotechnological production of carotenoids in microorganisms. Appl Microbiol Biot. 60(1-2), 1-11.
27. Lei, A.P., Chen, H., Shen, G.M., Hu, Z.L., Chen, L., Wang, J.X., 2012. Expression of fatty acid synthesis genes and fatty acid accumulation in *Haematococcus pluvialis* under different stressors. Biotechnol Biofuels. 5, 18.
28. Lim, D.K.Y., Schuhmann, H., Thomas-Hall, S.R., Chan, K.C.K., Wass, T.J., Aguilera, F., Adarme-Vega, T.C., Dal'Molin, C.G.O., Thorpe, G.J., Batley, J., Edwards, D., Schenk, P.M., 2017. RNA-Seq and metabolic flux analysis of *Tetraselmis* sp. M8 during nitrogen starvation reveals a two-stage lipid accumulation mechanism. Bioresour Technol. 244 (2), 1281-1293.
29. Lorenz, R.T., Cysewski, G.R., 2000. Commercial potential for *Haematococcus* microalgae as a natural source of astaxanthin. Trends Biotechnol. 18(4), 160-167.
30. Lung, S.C., Weselake, R.J., 2006. Diacylglycerol acyltransferase: A key mediator of plant triacylglycerol synthesis. Lipids. 41(12), 1073-1088.
31. Miao, F.P., Lu, D.Y., Li, Y.G., Zeng, M.T., 2006. Characterization of astaxanthin esters in *Haematococcus pluvialis* by liquid chromatography-atmospheric pressure chemical ionization mass spectrometry. Anal Biochem. 352(2), 176-181.
32. Mulders, K.J.M., Weesepoel, Y., Bodenes, P., Lamers, P.P., Vincken, J.P., Martens, D.E., Gruppen, H., Wijffels, R.H., 2015. Nitrogen-depleted *Chlorella zofingiensis* produces astaxanthin, ketolutein and their fatty acid esters: a carotenoid metabolism study. J Appl Phycol. 27(1), 125-140.
33. Nguyen, H.M., Cuine, S., Beyly-Adriano, A., Legeret, B., Billon, E., Auroy, P., Beisson, F., Peltier, G., Li-Beisson, Y., 2013. The green microalga *Chlamydomonas reinhardtii* has a single omega-3 fatty acid desaturase that localizes to the chloroplast and impacts both plastidic and extraplastidic membrane lipids. Plant Physiol. 163(2), 914-928.
34. Nymark, M., Valle, K.C., Brembu, T., Hancke, K., Winge, P., Andresen, K., Johnsen, G., Bones, A.M., 2009. An integrated analysis of molecular acclimation to high light in the marine diatom *Phaeodactylum tricornutum*. Plos One. 4(11), e7743.
35. Parvini, F., Sicardo, M.D., Hosseini-Mazinani, M., Martinez-Rivas, J.M., Hernandez, M.L., 2016. Transcriptional analysis of stearoyl-Acyl carrier protein desaturase genes from olive (*Olea europaea*) in relation to the oleic acid content of the virgin olive oil. J Agric Food Chem. 64(41), 7770-7781.
36. Ramakers, C., Ruijter, J.M., Deprez, R.H.L., Moorman, A.F.M., 2003. Assumption-free analysis of quantitative real-time polymerase chain reaction (PCR) data. Neurosci Lett. 339(1), 62-66.
37. Schuhmann, H., Lim, D.K.Y., Schenk, P.M., 2014. Perspectives on metabolic engineering for increased lipid contents in microalgae. Biofuels. 3(1), 71-86.
38. Scibilia, L., Girolomoni, L., Berteotti, S., Alboresi, A., Ballottari, M., 2015. Photosynthetic response to nitrogen starvation and high light in *Haematococcus pluvialis*. Algal Res. 12, 170-181.

39. Shah, M.M.R., Liang, Y.M., Cheng, J.J., Daroch, M., 2016. Astaxanthin-producing green microalga *Haematococcus pluvialis*: from single cell to high value commercia products. Front Plant Sci. 7, 531.
40. Steinbrenner, J., Linden, H., 2003. Light induction of carotenoid biosynthesis genes in the green alga *Haematococcus pluvialis*: regulation by photosynthetic redox control. Plant Mol Biol. 52(2), 343-356.
41. Teo, C.L., Atta, M., Bukhari, A., Taisir, M., Yusuf, A.M., Idris, A., 2014. Enhancing growth and lipid production of marine microalgae for biodiesel production via the use of different LED wavelengths. Bioresour Technol. 162, 38-44.
42. Weesepoel, Y., Vincken, J.P., Pop, R.M., Liu, K., Gruppen, H., 2013. Sodiation as a tool for enhancing the diagnostic value of MALDI-TOF/TOF-MS spectra of complex astaxanthin ester mixtures from *Haematococcus pluvialis*. J Mass Spectrom. 48(7), 862-874.
43. Zhao, N., Zhang, Y., Li, Q.Q., Li, R.F., Xia, X.L., Qin, X.W., Guo, H.H., 2015. Identification and expression of a stearoyl-ACP desaturase gene responsible for oleic acid accumulation in *Xanthoceras sorbifolia* seeds. Plant Physiol Bioch. 87, 9-16.
44. Zhekisheva, M., Boussiba, S., Khozin-Goldberg, I., Zarka, A., Cohen, Z., 2002. Accumulation of oleic acid in *Haematococcus pluvialis* (Chlorophyceae) under nitrogen starvation or high light is correlated with that of astaxanthin esters. J Phycol. 38(2), 325-331.

Figure legends

Figure 1. Cell number, residual nitrate, and astaxanthin dry weight contents of *H. pluvialis* cultures under different LED lighting conditions. A, cell number of *H. pluvialis* from day 0 to day 8; B, residual nitrate of *H. pluvialis* cultures on day 0 and day 2 (nitrate replete); C, free astaxanthin content; D, astaxanthin monoesters content; E, astaxanthin diesters; F, total astaxanthin.

Figure 2. Fatty acid profile (mg g^{-1}, dry weight) of *H. pluvialis* under different LED lighting conditions. A, C16:0; B, C18:0; C, C18:1n9; D, C18:2n6; E, C18:3n3; F, C18:3n6; G, C20:4n6; H, SFA; I, MUFA; J, PUFA; K, TFA.

Figure 3. Gene expression of *H. pluvialis* astaxanthin biosynthesis pathway under different LED lighting conditions. N indicates nitrogen depletion, H indicates high light intensity, and B indicates blue LED. Upwards arrow means gene expression was upregulated, rightwards arrow means gene expression was unchanged, and downwards arrow means gene expression was downregulated.

Figure 4. Gene expression of *H. pluvialis* fatty acid biosynthesis pathway under different LED lighting conditions. N indicates nitrogen depletion, H indicates high light intensity, and B indicates blue LED. Upwards arrow means gene expression was upregulated, rightwards arrow means gene expression was unchanged, and downwards arrow means gene expression was downregulated.

Figure 5. Gene expression of *H. pluvialis* fatty acid degradation pathway under different LED lighting conditions. N indicates nitrogen depletion, H indicates high light intensity, and B indicates blue LED. Upwards arrow means gene expression was upregulated, rightwards arrow means gene expression was unchanged, and downwards arrow means gene expression was downregulated.

Figure 6. Gene expression of *H. pluvialis* fatty acid degradation pathway under different LED lighting conditions. Acyl-CoA synthetase (ACSase); Acyl-CoA oxidase (ACO); Enoyl-CoA hydratase (ECH); Hydroxyacyl- CoA dehydrogenase (HAD); Ketoacyl- CoA thiolase (KAT). N indicates nitrogen depletion, H indicates high light intensity, and B indicates blue LED. Upwards arrow means gene expression was upregulated, rightwards arrow means gene expression was unchanged, and downwards arrow means gene expression was downregulated.

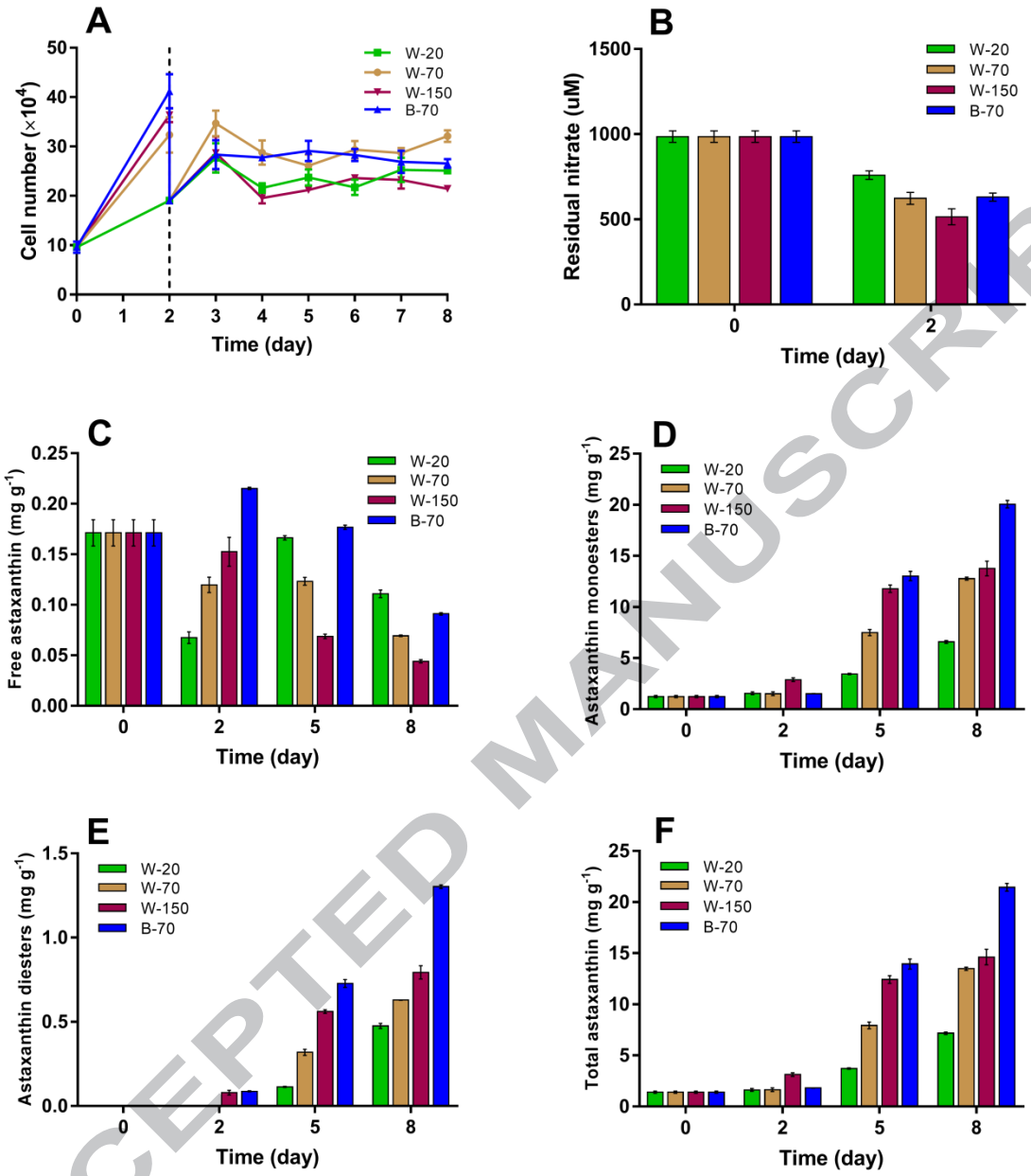

Fig. 1. Cell number, residual nitrate, and astaxanthin dry weight contents of *H. pluvialis* cultures under different LED lighting conditions. A, cell number of *H. pluvialis* from day 0 to day 8; B, residual nitrate of *H. pluvialis* cultures on day 0 and day 2 (nitrate replete); C, free astaxanthin content; D, astaxanthin monoesters content; E, astaxanthin diesters; F, total astaxanthin.

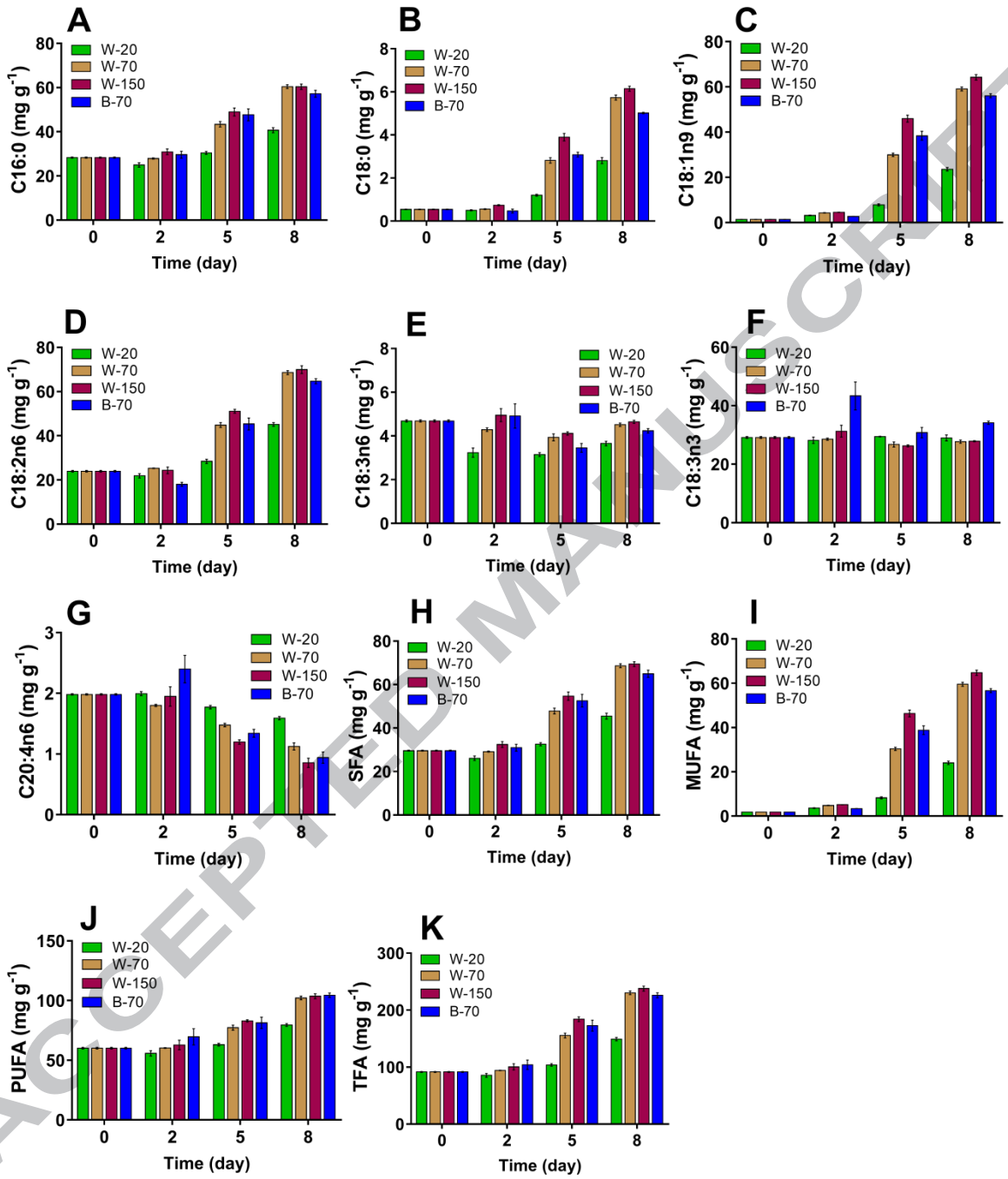

Fig. 2. Fatty acid profile (mg g^{-1}, dry weight) of *H. pluvialis* under different LED lighting conditions. A, C16:0; B, C18:0; C, C18:1n9; D, C18:2n6; E, C18:3n3; F, C18:3n6; G, C20:4n6; H, SFA; I, MUFA; J, PUFA; K, TFA.

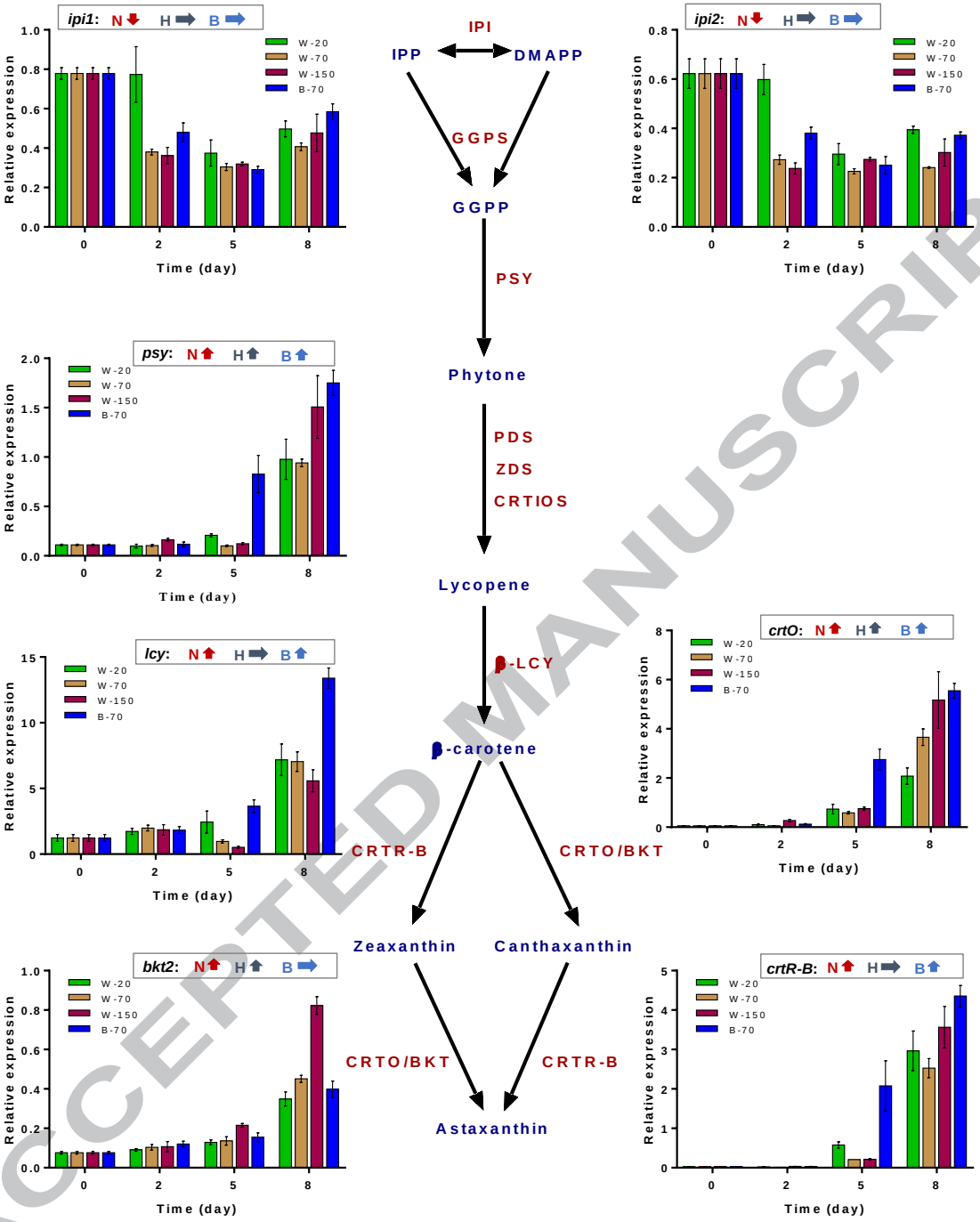

Fig. 3. Gene expression of *H. pluvialis* astaxanthin biosynthesis pathway under different LED lighting conditions. N indicates nitrogen depletion, H indicates high light intensity, and B indicates blue LED. Upwards arrow means gene expression was upregulated, rightwards arrow means gene expression was unchanged, and downwards arrow means gene expression was downregulated.

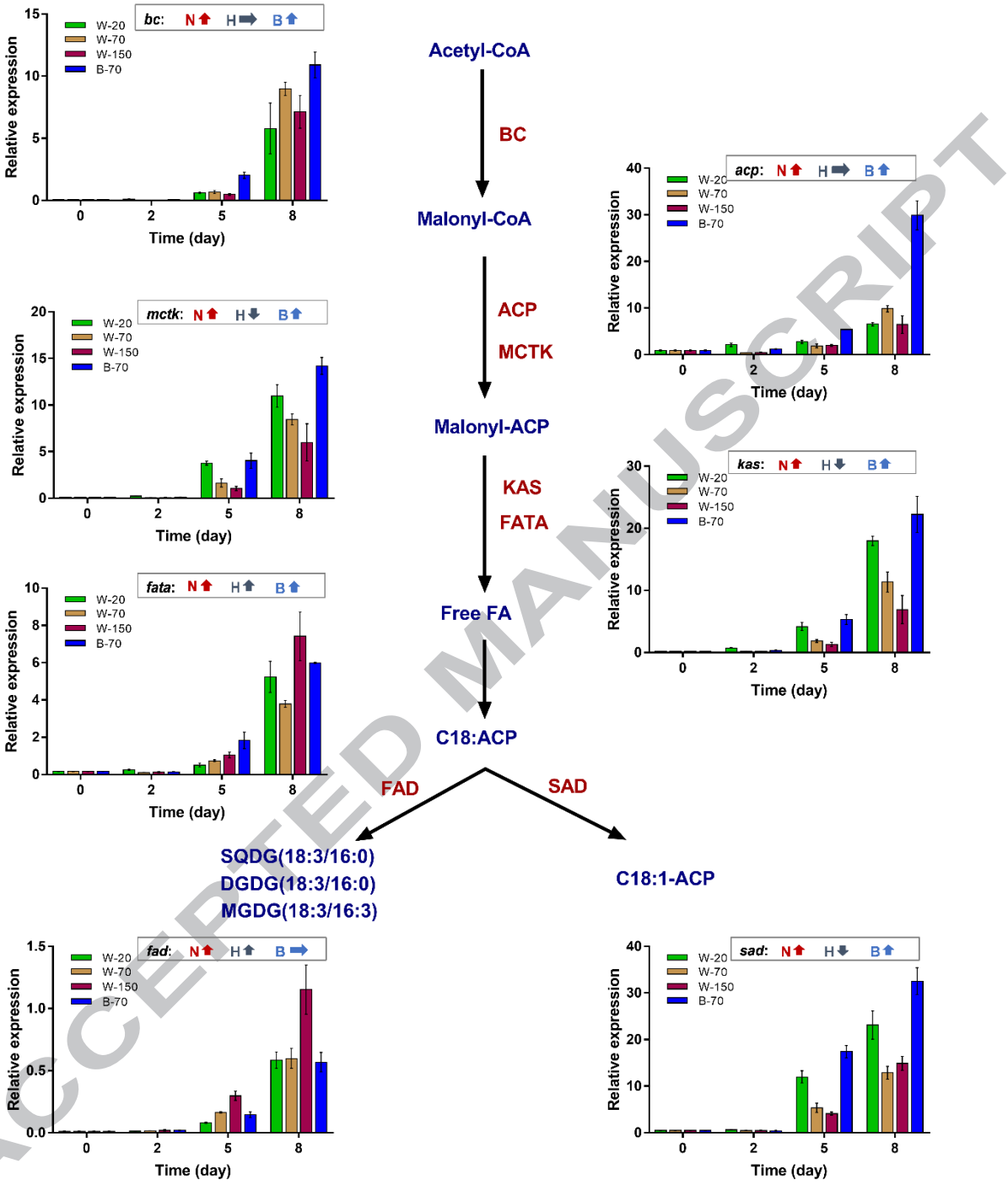

Fig. 4. Gene expression of *H. pluvialis* fatty acid biosynthesis pathway under different LED lighting conditions. N indicates nitrogen depletion, H indicates high light intensity, and B indicates blue LED. Upwards arrow means gene expression was upregulated, rightwards arrow means gene expression was unchanged, and downwards arrow means gene expression was downregulated.

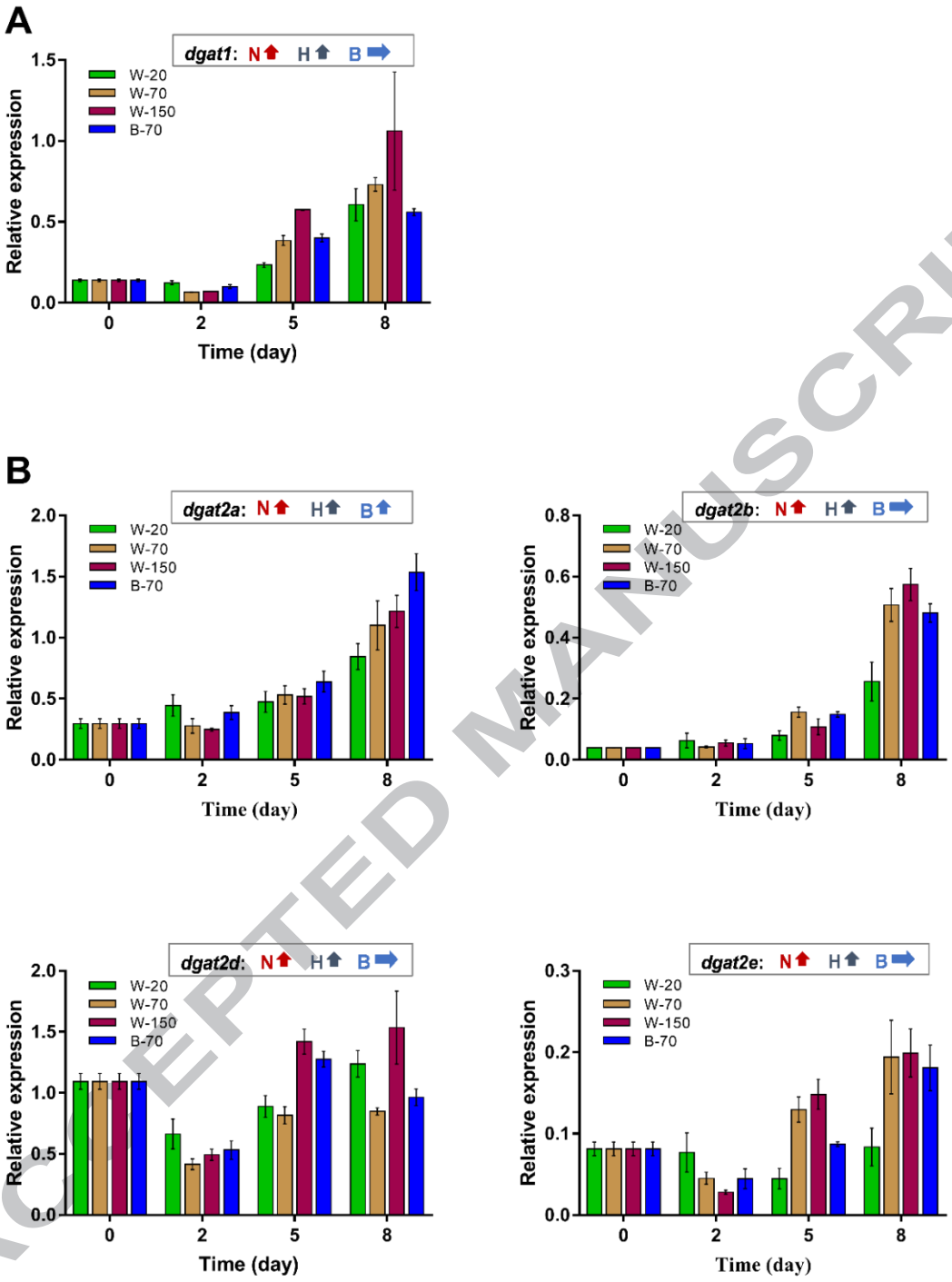

Fig. 5. Gene expression of *H. pluvialis* fatty acid degradation pathway under different LED lighting conditions. N indicates nitrogen depletion, H indicates high light intensity, and B indicates blue LED. Upwards arrow means gene expression was upregulated, rightwards arrow means gene expression was unchanged, and downwards arrow means gene expression was downregulated.

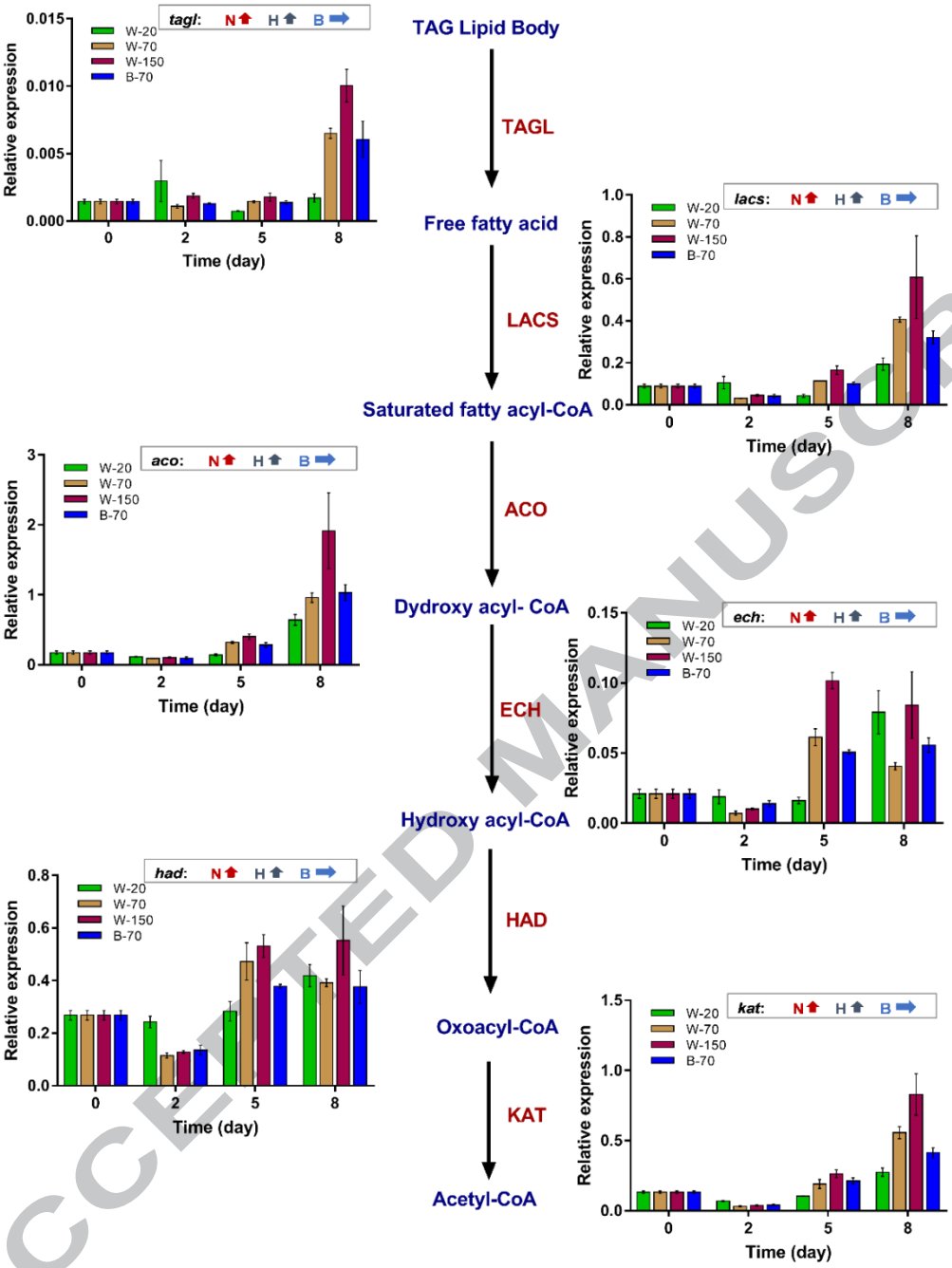

Fig. 6. Gene expression of *H. pluvialis* fatty acid degradation pathway under different LED lighting conditions. Acyl-CoA synthetase (ACSase); Acyl-CoA oxidase (ACO); Enoyl-CoA hydratase (ECH); Hydroxyacyl- CoA dehydrogenase (HAD); Ketoacyl- CoA thiolase (KAT). N indicates nitrogen depletion, H indicates high light intensity, and B indicates blue LED. Upwards arrow means gene expression was upregulated, rightwards arrow means gene expression was unchanged, and downwards arrow means gene expression was downregulated.

Highlights

- LEDs provide useful tools to stimulate *Haematococcus* astaxanthin biosynthesis.
- High intensity white and blue LED significantly increased astaxanthin content.
- Total fatty acid content was induced by high intensity white LED.
- Astaxanthin and fatty acid biosynthesis genes are regulated by different LEDs.
- Five *H. pluvialis dgat* genes were identified and *dgat2a* was induced by blue LED.

Graphical abstract

Graphical abstract

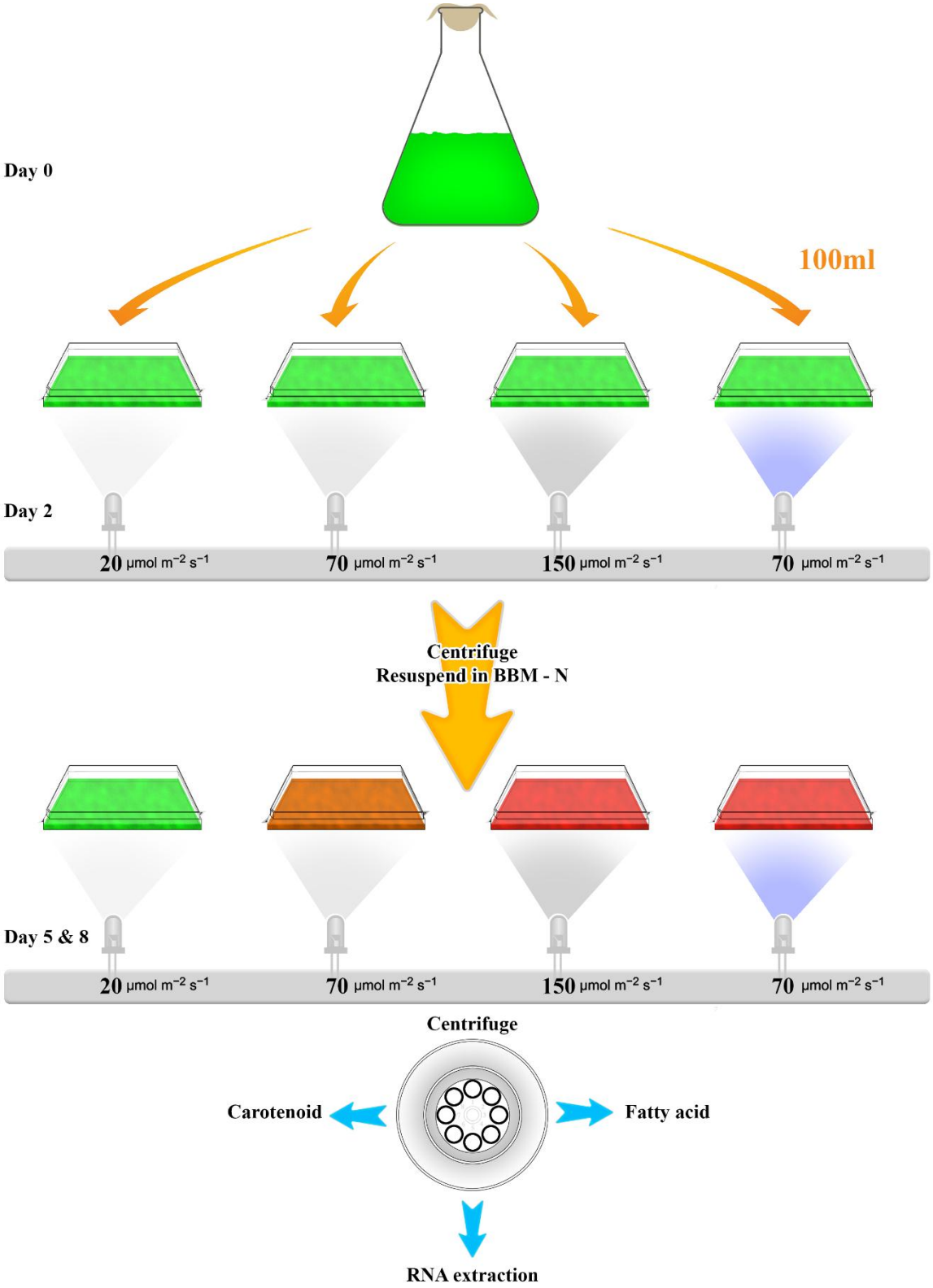
Day 0
100ml
Day 2
20 μmol m⁻² s⁻¹
70 μmol m⁻² s⁻¹
150 μmol m⁻² s⁻¹
70 μmol m⁻² s⁻¹
Centrifuge
Resuspend in BBM - N
Day 5 & 8
20 μmol m⁻² s⁻¹
70 μmol m⁻² s⁻¹
150 μmol m⁻² s⁻¹
70 μmol m⁻² s⁻¹
Centrifuge
Carotenoid
Fatty acid
RNA extraction